Controlling photon transport in the single-photon weak-coupling regime of cavity optomechanics

Wen-Zhao Zhang, Jiong Cheng, Jing-Yi Liu, and Ling Zhou*

School of Physics and Optoelectronic Technology, Dalian University of Technology, Dalian 116024, People's Republic of China

(Received 22 March 2015; published 29 June 2015)

We study the photon statistics properties of few-photon transport in an optomechanical system where an optomechanical cavity couples to two empty cavities. By analytically deriving the one- and two-photon currents in terms of a zero-time-delayed two-order correlation function, we show that a photon blockade can be achieved in both the single-photon strong-coupling regime and the single-photon weak-coupling regime due to the nonlinear interacting and multipath interference. Furthermore, our systems can be applied as a quantum optical diode, a single-photon source, and a quantum optical capacitor. It is shown that this the photon transport controlling devices based on photon antibunching does not require the stringent single-photon strong-coupling condition. Our results provide a promising platform for the coherent manipulation of optomechanics, which has potential applications for quantum information processing and quantum circuit realization.

DOI: 10.1103/PhysRevA.91.063836 PACS number(s): 42.50.Wk, 42.50.Ex, 07.10.Cm

I. INTRODUCTION

The nonlinear effect is a potential resource for quantum information processing [1]. For example, the photon blockade resulting from the nonlinearity is employed in single-photon (few-photon) transmission control [2] and optical state truncation [3]. Similarly, the photon blockade is also an important feature in many quantum device designs such as the fast two-qubit controlled-NOT gate [4], efficient quantum repeaters [5], single-photon transistors [6], and optical quantum computers [7]. The rectifying device related to nonlinearity is the key device to information processing in integrated circuits [8]. Considerable effort has been made to investigate optical diodes [9]. Various possible solid-state optical diodes have been proposed, for example, the diodes from standard bulk Faraday rotators [10], integrated on a chip [11], realized in an optoacoustic fiber [12], and from a moving photonic crystal [13]. A kind of optical diode based on the photon blockade effect also has been proposed, including a photonic diode by a nonlinear-linear junction of coupled resonators [14] and an optical diode of two semiconductor microcavities coupled via $\chi^{(2)}$ nonlinearities [15].

The nonlinear interaction between optical and mechanical modes arising from the radiation pressure force in optomechanical (OM) systems exhibits many interesting nonlinear effects such as a photon (phonon) blockade [16,17], optomechanical-induced transparency [18,19], and Kerr nonlinearity [20,21]. Cavity optomechanics has received significant attention in both fundamental experiments [22,23] and sensing applications [24,25]. Currently, experimental techniques of cavity optomechanics are still in the single-photon weak-coupling regime [26] ($g^2 < \kappa\omega_m$), however it draws relatively few works on control devices in quantum information processing because a prerequisite of strong nonlinearity is required [27,28]. In order to utilize the nonlinearity of the OM system in quantum information control, much attention has been paid to the photon blockade in OM systems, including quadratically coupled OM systems [29], hybrid electro-optomechanical systems [30], and ultrastrong optomechanics [31], where the single-photon strong-coupling condition is required. Reference [32] has shown that strong photon antibunching can be achieved in two coupled cavities with weak Kerr nonlinearity, which motivate us try to achieve a strong nonlinear effect in an OM system in the single-photon weak-coupling regime. In this paper we propose a scheme to realize an optical diode with the optomechanical cavity coupled to two cavities. This scheme does not require the stringent condition that the single-photon optomechanical coupling strength g is on the order of the mechanical resonance frequency ω_m [16] or the coupling strength g is larger than the cavity decay rate κ [29]. Our results show that a photon blockade can be achieved in both the single-photon strong-coupling regime and the single-photon weak-coupling regime because of the nonlinearity and multipath interference. By examining the second-order correlation function, rectifying factor $\mathcal{R}$, and transport efficiency $\mathcal{T}$, we exhibit the characteristics of our system as a photonic diode. Meanwhile, the single-photon transport can be controlled by tuning the frequency of the cavities in the single-photon strong-coupling regime. Surprisingly, by pumping two sides of the system (cavity L and R), the device will embody some characteristics like the capacitor: photon storage and release (charge and discharge) and filtering of the photon frequency.

The paper is organized as follows. In Sec. II we introduce the system and eigensystem of Hamiltonian. We discuss photon transport control in the cavity optomechanical system, such as a diode and a capacitor, in Sec. III. A summary given in Sec. IV.

II. MODEL AND HAMILTONIAN

We consider a compound optomechanical system in which a cavity with a movable mirror is coupled with two cavities (L and R) with the coupling constant J_L and J_R (see Fig. 1). The system described by the Hamiltonian $H = H_{\rm sys} + H_{\rm pump}$. By setting $\hbar = 1$, the Hamiltonian $H_{\rm sys}$ reads

$$H_{\rm sys} = \sum_{j=L,C,R} \omega_l a_j^\dagger a_j + \omega_m b^\dagger b + g(b^\dagger + b)a_C^\dagger a_C + (J_L a_L^\dagger a_C + J_R a_R^\dagger a_C + \text{H.c.}), \quad (1)$$

*zhlhxn@dlut.edu.cn

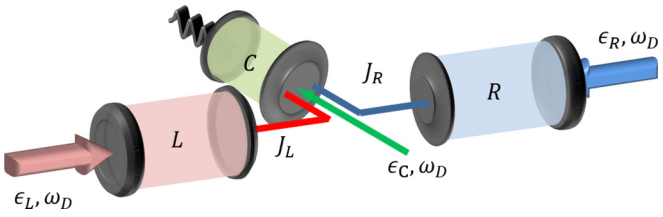

FIG. 1. (Color online) Schematic of the cavity optomechanical system coupled with two cavities. Cavities L, R, and C all can be driven by the laser field with the same frequency.

where a_C, a_L, and a_R are the annihilation operators for the photon mode of cavities C, L, and R with frequencies ω_C, ω_L, and ω_R, respectively; b is the phonon annihilation operator of the mechanical mode for the mirror with frequency ω_m; and g denotes the coupling strength of the radiation pressure. The cavity modes are driven by the laser with the same frequency ω_D, which can be described by $H_{\rm pump} = i\sum_{j=L,C,R}\varepsilon_j(a_j^\dagger e^{-i\omega_D t} - \text{H.c.})$. In the rotating frame with $H_0 = \sum_{j=L,C,R}\omega_D a_j^\dagger a_j$, we obtain

$$\begin{aligned} H_S = &\sum_{j=L,C,R}\Delta_j a_j^\dagger a_j + \omega_m b^\dagger b + g(b^\dagger + b)a_C^\dagger a_C \\ &+ (J_L a_L^\dagger a_C + J_R a_R^\dagger a_C + \text{H.c.}) \\ &+ \sum_{j=L,C,R}\varepsilon_j(a_j^\dagger + a_j), \end{aligned} \tag{2}$$

where $\Delta_j = \omega_j - \omega_D$ ($j = L,C,R$) is the detuning between the driving field and the jth cavity frequency, respectively. For this cascade configuration, cavities L and R are used as input and output ports on the sides L and R. In this case, the optomechanical cavity, as an assisted cavity, provides an intrinsically nonlinear interaction.

We assume that the cavities (L and R) incoherently dissipate at rates κ_l ($l = L,R$) determined by the openness of the output channels and only classical driving fields are added to the quantum vacuum of the system. Then, according to the standard input-output relation [33], the average output current (or photon stream) as the number of quanta emitted at time t from each cavity can be formally given by

$$Q_l(t) = \kappa_l \text{Tr}[a_l^\dagger a_l \rho(t)] \quad (l = L,R), \tag{3}$$

where ρ is the density operator of system. The evolution of the density operator ρ for the Hamiltonian H_S can be described by the master equation

$$\begin{aligned} \dot\rho = &-i[H_S,\rho] + \sum_{j=L,C,R}\frac{\kappa_j}{2}\mathcal{D}[a_j]\rho + \frac{\gamma}{2}(n_{th}+1)\mathcal{D}[b]\rho \\ &+ \frac{\gamma}{2}n_{th}\mathcal{D}[b^\dagger]\rho, \end{aligned} \tag{4}$$

where κ_j and γ are the cavity and mechanical energy decay rates, respectively, $n_{th} = [\exp(\omega_m/k_B T_M - 1)]^{-1}$ is the average thermal occupancy number of the oscillator, and $\mathcal{D}[o] = 2o\rho o^\dagger - o^\dagger o\rho - \rho o^\dagger o$ is the Lindblad dissipation superoperator.

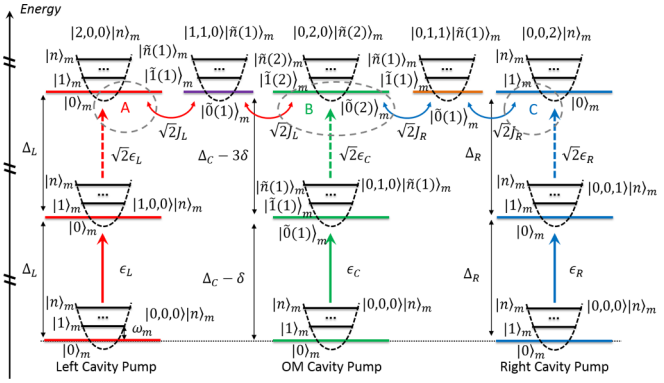

FIG. 2. (Color online) Eigensystem of the Hamiltonian H_S in the zero-, one-, and two-photon cases. Subareas A, B, and C denote multipath interference in the system.

The eigenequation of the Hamiltonian $H_{om} = \omega_m b^\dagger b + \Delta_C a^\dagger a + g(b^\dagger + b)a^\dagger a$ can be expressed as

$$H_{om}|s\rangle_C|\tilde n(s)\rangle_m = E_{s,n}|s\rangle_C|\tilde n(s)\rangle_m,$$

where the eigenvalues are

$$E_{s,n} = s\Delta_C + n\omega_m - s^2\delta,$$

with $\delta = \frac{g^2}{\omega_m}$, and the eigenstate

$$|\tilde n(s)\rangle = e^{g(b-b^\dagger)/\omega_m}|n\rangle \tag{5}$$

is the displaced number state. The eigensystem of the Hamiltonian H_S in the zero-, one-, and two-photon cases is shown in Fig. 2. We noticed that the energy levels for the optomechanical cavity (middle green line) will obtain a shift $s^2\delta$ caused by the nonlinearity interacting with a frequency red (blue) detuning from the resonator resonance. This nonlinear shift can lead to bunched or antibunched photons in the OM cavity (details are given in Sec. III C). This nonlinear effects also can appear in other cavities because of the couplings J_L and J_R. Especially in the single-photon strong-coupling regime $g/\kappa \gg 1$, a photon blockade appears in the system, i.e., the probability of two photons inside the cavity is largely suppressed due to the energy restriction.

The interference between multiple paths for two-photon excitation in cavities is partially responsible for the photon antibunching effect shown in the subareas A, B, and C of the eigensystem diagram. For area A, the two photons in cavity L with the state $|2,0,0\rangle|n\rangle_m$ have two excitation paths: One is direct excitation from a low level in cavity L with the state $|1,0,0\rangle|n\rangle_m$ and the other is the tunneling from the OM cavity to the left cavity with the state $|1,1,0\rangle|\tilde n\rangle_m$. The destructive interference between the two paths reduces the probability of two-photon excitation in the cavity as well as in areas B and C. When the probability is equal to zero, an unconventional photon blockade [32,34,35] appears in the cavity with no requirement of a strong nonlinear coupling coefficient g (even $g/\kappa < 1$). Therefore, the compound optomechanical system can work as a single-photon control device in OM single-photon weak- and strong-coupling regimes, which will be discussed in detail in the next section.

III. PHOTONS TRANSPORT CONTROL IN THE CAVITY OPTOMECHANICAL SYSTEM

A. Optomechanical optical diode

When the nonlinear effect for the right-going k waves is different from that for the left-going $-k$ waves, i.e., the nonlinearity of the composite system is asymmetric, the rectification of one-dimensional photon transport can be controlled. The one-way transport is called an optical diode [9]. In this section we show that our compound system can work as a photonic diode.

We are interested in the statistical property of photons and its control. Usually, the frequency of the mechanical oscillator is larger than the strength of coupling of the radiation pressure, i.e., $\omega_m \gg g$. For simplicity, we can adiabatically eliminate the degree of the oscillators. Including the decay rate of the cavities, we have a non-Hermitian effective Hamiltonian

$$H_{\text{eff}} = \sum_{j=L,C,R} [(\Delta_j - i\kappa_j/2)a_j^\dagger a_j + \varepsilon_j(a_j^\dagger + a_j)] - i\sum_{j=L,C,R} \frac{\kappa_j}{2} a_j^\dagger a_j - \delta a_C^\dagger a_C - \delta a_C^\dagger a_C^\dagger a_C a_C + (J_L a_L^\dagger a_C + J_R a_R^\dagger a_C + \text{H.c.}). \quad (6)$$

We assume that the general state is

$$|\psi(t)\rangle = C_0(t)|\emptyset\rangle + \sum_{j=L,C,R} C_j(t)a_j^\dagger|\emptyset\rangle + \sum_{i,j=L,C,R} \frac{1}{2} C_{ij}(t)a_i^\dagger a_j^\dagger|\emptyset\rangle. \quad (7)$$

Under weak pumping conditions, we have [32]

$$C_0 \gg C_j \gg C_{ij}.$$

Under this condition, one can obtain the steady-state solution of the probability amplitudes (see the Appendix).

The effect of quantum nonlinear features can be characterized by the second-order correlation function with zero-time delay

$$g_j^{(2)}(0) = \frac{\langle a_j^{\dagger 2} a_j^2 \rangle}{\langle a_j^\dagger a_j \rangle^2}, \quad j = L,R,C. \quad (8)$$

We notice that $g_j^{(2)}(0) < 1$ indicates photon antibunching and $g_j^{(2)}(0) > 1$ indicates photon bunching. Antibunching corresponds to a reduced probability of two photons in the cavity at a given time, which is the opposite of bunching. The probability of two photons in the cavity will equal zero if $g_j^{(2)}(0) \approx 0$ (photon blockade). For simplify, we set $\kappa_L = \kappa_R = \kappa_C = \kappa$ and $\alpha_j = \Delta_j - i\kappa/2$ $(j = L,C,R)$. If $\alpha_L = \alpha_R = \alpha$, $\varepsilon_L = \varepsilon$, and $\varepsilon_C, \varepsilon_R = 0$, i.e., the system is only pumped on the left cavity with the magnitude ε, the photon second-order correlation function with no time delay in the left cavity can be obtained

$$g_L^{(2)}(0) = \left| \frac{J_R^4 K_2 + (J_L^2 - J_R^2)K_1 F_2}{(J_L^2 + J_R^2)K_2 - K_1 F_2} - F_1 \right|^2 \left| \frac{J_L^2 + J_R^2 - F_1}{(J_R^2 - F_1)^2} \right|^2, \quad (9)$$

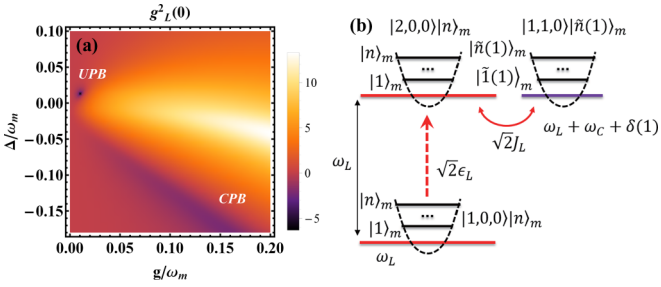

FIG. 3. (Color online) (a) Zero-time second-order correlation $g_L^{(2)}(0)$ as a function of the coupling strength g and the driving detuning Δ (on a logarithmic scale). Other parameters are $J_L/\omega_m = 0.5$, $J_R/\omega_m = 0.01$, and $\kappa/\omega_m = 0.036$. (b) Eigensystem of two-excitation path interference in cavity L.

where $K_n = \alpha + \alpha_C + n\delta$ and $F_n = \alpha(\alpha_C + n\delta)$ $(n = 1,2)$. Setting $\Delta_L = \Delta_R = \Delta_C = \Delta$, we plot logarithmic $g_L^{(2)}(0)$ as a function of Δ and g in Fig. 3(a). Here $g_L^{(2)}(0) \approx 0$ represents a photon blockade, corresponding to the dark areas, which appears in two areas. One is achieved in the bottom right area in Fig. 3(a) with large values of the coupling rate g, which means that the photon blockade results from the nonlinear effects of radiation pressure. We call it a conventional photon blockade (CPB). The other appears in the top left area with small values of g but strict limitations on other parameters, which means that it results from the two-path interference. The interference between the two excitation paths (one exciton is from its own exciton and the other is the jumping from its neighbor) is illustrated in Fig. 3(b). Because of the destructive interference, the photon blockade phenomenon also occurs, called an unconventional photon blockade (UPB).

We now show the photon statistics properties and control of the photon transport by comparing the analytical solution with the numerical results via solving the master equation (4). For the conventional photon blockade, the larger the ratio of g/κ, the stronger the effect of the blockade, shown in Fig. 4(a). The corresponding detuning frequency can be derived from Eq. (9). As shown in Fig. 4(b), the strong photon antibunching can be obtained even if $g/\kappa < 1$.

In order to describe the characteristics of unidirectional energy transport we define the rectifying factor $\mathcal{R}$ and transport efficiency $\mathcal{T}$ as the normalized difference between the output currents when the system is pumped through the left and right resonators (indicated by the wave vectors k and $-k$, respectively) [14]

$$\mathcal{R} = \frac{Q_R[k] - Q_L[-k]}{Q_R[k] + Q_L[-k]}, \quad (10)$$

$$\mathcal{T}_L = \frac{Q_R[k]}{Q_R[k] + Q_L[k]}, \quad (11)$$

$$\mathcal{T}_R = \frac{Q_L[-k]}{Q_R[-k] + Q_L[-k]}, \quad (12)$$

where $\mathcal{R} = -1$ indicates maximal rectification with enhanced transport to the left (left rectification), $\mathcal{R} = 0$ indicates no rectification because $Q_R[k] = Q_L[-k]$, and $\mathcal{R} = 1$ indicates maximal rectification with transport to the right (right rectification). In our system, cavity L and cavity R are both linear

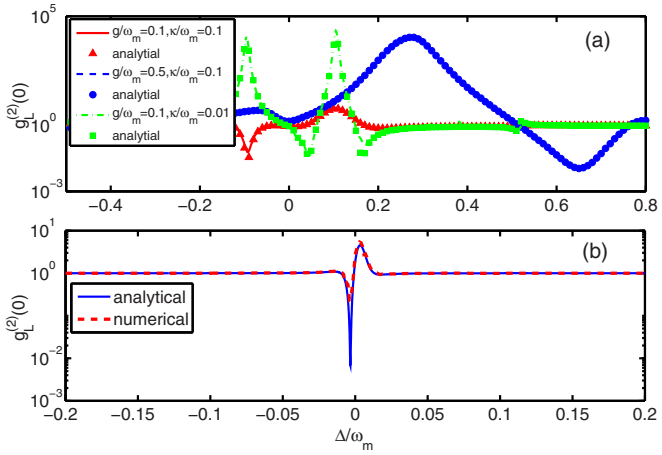

FIG. 4. (Color online) Equal-time second-order correlation $g_L^{(2)}(0)$ as a function of the coupling strength g and the driving detuning Δ with $\Delta_L = \Delta_C = \Delta$ and $\Delta_R = \Delta + \Delta_{LR}$. Other parameters are (a) $J_L/\omega_m = 0.5$, $J_R/\omega_m = 0.1$, and $\Delta_{LR} = 0$ and (b) $J_L/\omega_m = 0.1$, $J_R/\omega_m = 0.01$, $g/\omega_m = 0.01$, $\kappa/g = 1.3$, and $\Delta_{LR} = 0.1$ (other groups of parameters can be obtained by solving $g_L^{(2)}(0) = 0$ in the single-photon weak-coupling regime).

cavities. Therefore, there is no rectification ($\mathcal{R} = 0$) when only driving the left or right cavity (no asymmetric nonlinear effect).

We discuss the rectification effect in the conventional blockade regime ($\omega_m > g > \kappa$) shown in Fig. 5. When $\frac{\Delta}{\omega_m}$ is around -0.02, $\mathcal{R} \approx 1$, which indicates that the system allows photon transfer from left to right $L \to R$ only and the transfer is prohibited from right to left $R \to L$, the photon number from the left-going $-k$ field is equal to zero on side L. Similarly, when $\frac{\Delta}{\omega_m}$ is around 0.005, $\mathcal{R} = -1$, which only allows the transport from right to left $R \to L$ and $N_R(k) = 0$. For $\frac{\Delta}{\omega_m}$ around -0.005, $\mathcal{R} = 0$, the photon number from the left-going $-k$ field is equal to the photon number from the right-going k field $N_L(-k) = N_R(k)$. If $g < \kappa < \omega_m$

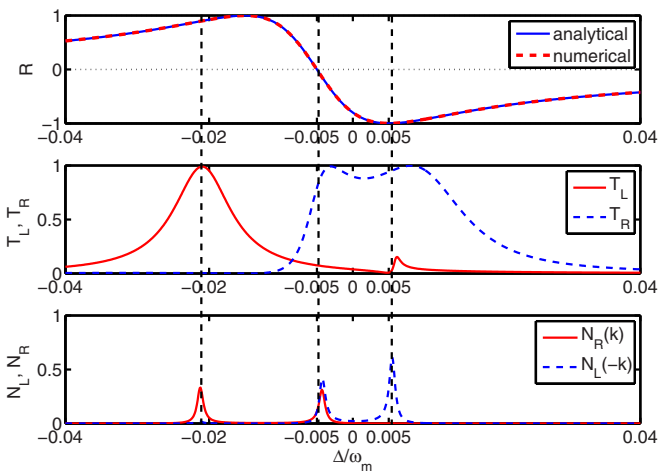

FIG. 5. (Color online) Rectifying factor, transport efficiency, and excitation number in the cavity as a function of the driving detuning Δ with $\Delta_L = \Delta_C = \Delta$ and $\Delta_R = \Delta + \Delta_{LR}$. Other parameters are $g/\omega_m = 5\times10^{-3}$, $J_L/\omega_m = 5\times10^{-3}$, $J_R/\omega_m = 5\times10^{-3}$, $\kappa/g = 0.2$, and $\Delta_{LR}/\omega_m = 2\times10^{-2}$.

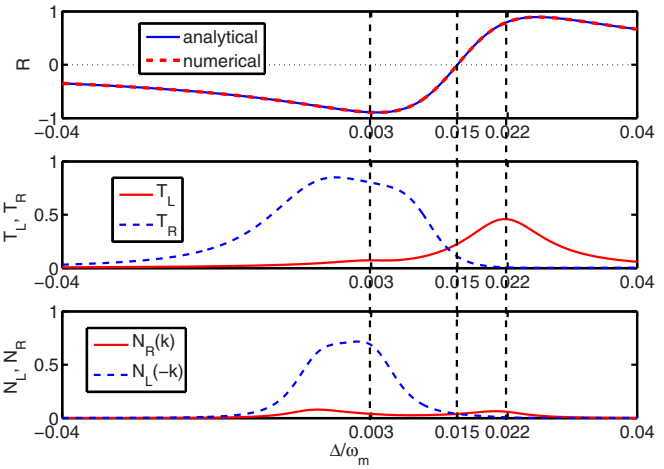

FIG. 6. (Color online) Rectifying factor, transport efficiency, and excitation number in the cavity as a function of the driving detuning Δ with $\Delta_L = \Delta_C = \Delta$ and $\Delta_R = \Delta + \Delta_{LR}$. Other parameters are $g/\omega_m = 5\times10^{-3}$, $\kappa/g = 2$, $J_L/\omega_m = 5\times10^{-3}$, $J_R/\omega_m = 5\times10^{-3}$, and $\Delta_{LR}/\omega_m = -2\times10^{-2}$.

(unconventional blockade regime), shown in Fig. 6, one can obtain $\mathcal{R} \approx 1$ when $\frac{\Delta}{\omega_m} = 0.022$. We also can see $\mathcal{R} = 0$ for $\frac{\Delta}{\omega_m} = 0.015$ and $\mathcal{R} \approx -1$ for $\frac{\Delta}{\omega_m} = 0.003$. Therefore, we can conclude that whether $\omega_m > g > \kappa$ or $g < \kappa < \omega_m$, by tuning the frequencies of the cavities R and L, one can adjust (or switch) rectification and two-way transport.

B. Single-photon source

The photon blockade effect allows only single-photon transmission through the system. Now we show that our device can work as a single-photon source. The system is only driven from the left or right cavity, i.e., $\varepsilon_L = \varepsilon$, $\varepsilon_R = \varepsilon_C = 0$ or $\varepsilon_R = \varepsilon$, $\varepsilon_L = \varepsilon_C = 0$. The mean occupation photon numbers

$$N_R(k) = N_L(-k) = \left| \frac{J_L J_R \varepsilon}{J_R^2 \alpha_L + \alpha_R \left[J_L^2 - \alpha_L(\alpha_C + \delta) \right]} \right|^2. \quad (13)$$

As shown in Fig. 7, the system only allows single-photon transport whether the light is from the left or right when $g_R^{(2)}(k) \approx g_L^{(2)}(-k) \approx 0$. The transport efficiency $\mathcal{T}_L = \mathcal{T}_R \approx 0.5$, which means that the output of the system is in a single-photon state if the input is in a two-photon state. Under this condition, the device can control the single-photon transport in the channel or work as a single-photon source. This kind of device can only work in the single-photon strong-coupling regime ($g/\kappa > 1$) because there is no multipath interference in output ports. We also notice that $\mathcal{R} \equiv 0$ even if $\alpha_L \neq \alpha_R$ and $J_L \neq J_R$. Achieving rectification requires $\varepsilon_C \neq 0$.

C. Optomechanical optical capacitor

As we have shown in Fig. 4, the photons in the left cavity exhibit antibunching, although the directly nonlinear interaction only appears in the OM cavity. Similar to the nonlinear shift 3δ in the OM cavity, the effective nonlinearity in

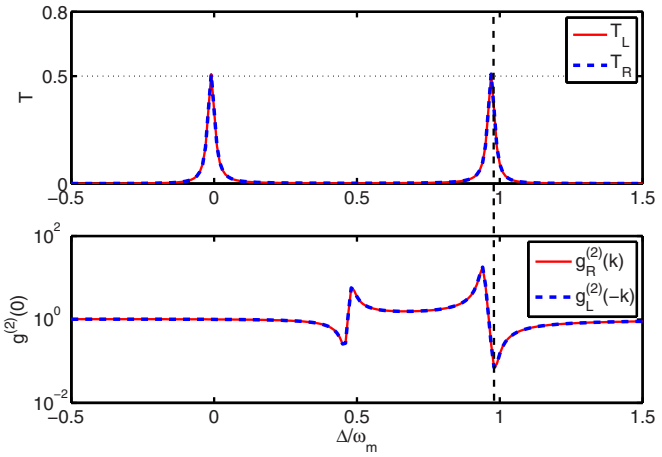

FIG. 7. (Color online) Transport efficiency and second-order correlation of output ports as a function of the driving detuning Δ with $\Delta_L = \Delta_R = \Delta$ and $\Delta_C = \Delta + \Delta_{LC}$. Other parameters are $g/\omega_m = 0.2$, $J_L/\omega_m = 0.1$, $J_R/\omega_m = 0.1$, $\kappa/g = 0.1$, and $\Delta_{LC}/\omega_m = -1$.

cavity L (R) can be equivalent to the resonance energy shift δ_L (δ_R). If cavities L and R both exhibit the photon antibunching effect due to the nonlinear shift and interference and the OM cavity exhibits the photon bunching effect, when we drive the cavities L and R, the photons can be stored in the OM cavity. Reversing the process, one can release the photons.

As shown in Figs. 8(a) and 8(c), the system is a symmetric structure. The field from the left and right cavities can be regarded as input k of the OM cavity, while the field from the OM cavity can be regarded as output $-k$ of the OM cavity. In Fig. 8(b), when $\{\omega_L,\omega_R\} > \omega_D$ and $\{\omega_L,\omega_R\} > \omega_C$, i.e., $\{\Delta_{LC},\Delta_{RC}\} < 0$ and $\{\Delta_L,\Delta_R\} > 0$, the nonlinear frequency shift in the left (right) cavity δ_L (δ_R) will increase the transition energy of the two-photon excitation, which means that the probability of the two-photon state will be suppressed and the photon exhibits antibunching in the cavity L (R). At the same time, the nonlinear shift in the OM cavity 3δ will diminish the detuning between the tunneling field ω_L (ω_R) and resonance frequency ω_C and the photon will exhibit bunching in the OM cavity. Especially for $\omega_D \approx \omega_C + 3\delta$, the OM cavity exhibits strong bunching due to the resonance absorption. Under this condition, the probability amplitude

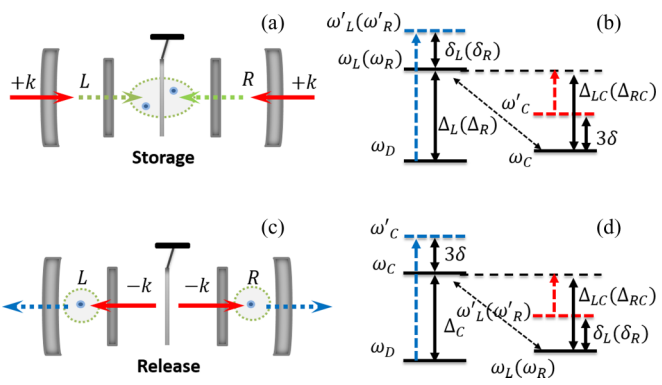

FIG. 8. (Color online) Pictorial representation and eigensystem of the photon storage and release process.

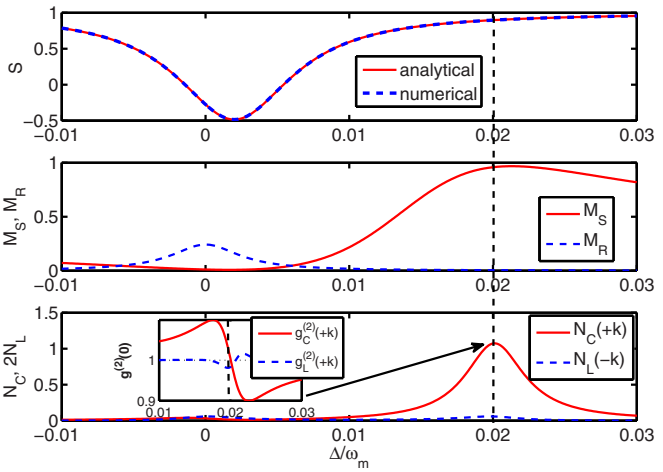

FIG. 9. (Color online) Storage factor, storage-release efficiency, and excitation number in the cavity as a function of the driving detuning Δ with $\Delta_L = \Delta_R = \Delta$ and $\Delta_C = \Delta + \Delta_{LC}$. Other parameters are $g/\omega_m = 5\times10^{-3}$, $\kappa/g = 1$, $J_L/\omega_m = J_R/\omega_m = 1\times10^{-3}$, and $\Delta_{LC}/\omega_m = -2\times10^{-2}$.

of photons in the OM cavity will be much larger than in the cavities L and R and photons can be stored in the OM cavity. Reversing the process, as shown in Fig. 8(d), when $\omega_C > \omega_D$ and $\omega_C > \{\omega_L,\omega_R\}$, i.e., $\{\Delta_{LC},\Delta_{RC}\} > 0$ and $\Delta_C > 0$, the nonlinear frequency shift 3δ will increase the transition energy of the two-photon excitation and the photon exhibits antibunching in the OM cavity. Meanwhile, the nonlinear shift in the left and right cavities δ_L and δ_R will diminish the detuning between the tunneling field ω_C and resonance frequency $\{\omega_L,\omega_R\}$ and the photon exhibits bunching in the left and right cavities. Under this condition, the photons can be released from the OM cavity.

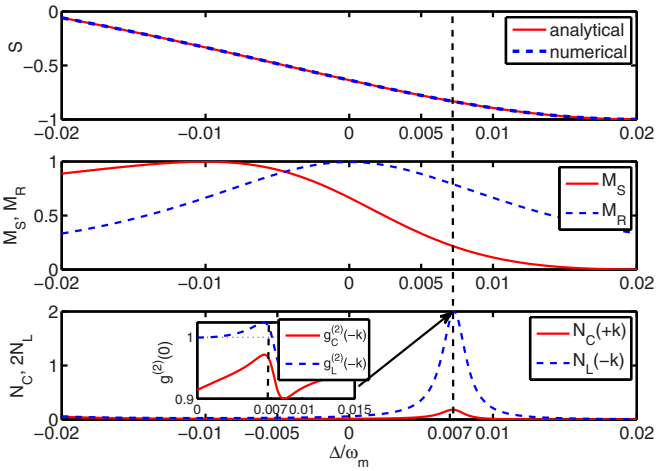

FIG. 10. (Color online) Storage factor, storage-release efficiency, and excitation number in the cavity as a function of the driving detuning Δ with $\Delta_L = \Delta_R = \Delta$ and $\Delta_C = \Delta + \Delta_{LC}$. Other parameters are $g/\omega_m = 1\times10^{-3}$, $\kappa/g = 2$, $J_L/\omega_m = J_R/\omega_m = 1\times10^{-2}$, and $\Delta_{LC}/\omega_m = 2\times10^{-2}$.

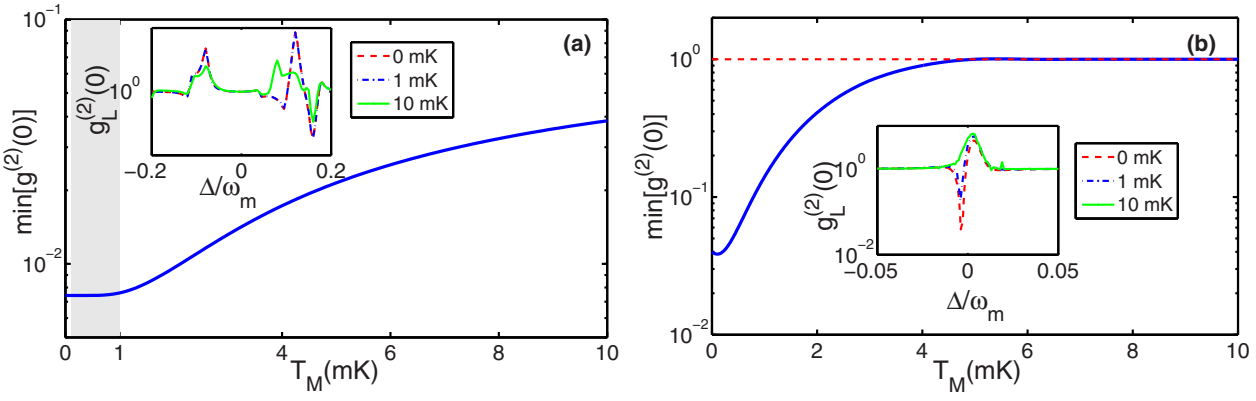

FIG. 11. (Color online) Minimum equal-time second-order correlation $g_L^{(2)}(0)$ as a function of mechanical bath temperature T_M with mechanical frequency $\omega_m = 0.1$ GHz and dissipation rate $\gamma = 1$ KHz. Other parameters are (a) $\Delta_L = \Delta_R = \Delta_C$, $g/\omega_m = 0.2$, $J_L = J_R = \omega_m/10$, and $\kappa/\omega_m = 10^{-2}$ and (b) $\Delta_L = \Delta_C$, $\Delta_{LR}/\omega_m = 0.1$, $g/\omega_m = 10^{-2}$, $J_L/\omega_m = 0.1$, $J_R/\omega_m = 0.01$, and $\kappa/g = 1.3$.

In order to describe the characteristics of energy storage and release we define the storage factor $\mathcal{S}$ and storage-release efficiency $\mathcal{M}$,

$$\mathcal{S} = \frac{Q_C[k] - Q_L[-k] - Q_R[-k]}{Q_C[k] + Q_L[-k] + Q_R[-k]}, \tag{14}$$

$$\mathcal{M}_S = \frac{Q_C[k]}{Q_C[k] + Q_L[k] + Q_R[k]}, \tag{15}$$

$$\mathcal{M}_R = \frac{Q_L[-k] + Q_R[-k]}{Q_C[-k] + Q_L[-k] + Q_R[-k]}, \tag{16}$$

where $\mathcal{S} = 1$ indicates maximal storage with the enhanced transport to the OM cavity, $\mathcal{S} = 0$ indicates no storage and release, and $\mathcal{S} = -1$ indicates maximal release with enhanced transport to the left and right cavities; $\mathcal{M}_S = 1$ or $\mathcal{M}_R = 1$ indicates that the photons are totally stored in or released from the OM cavity, respectively. For simplicity, we assume that all parameters of the cavities L and R are exactly the same in the following discussion. The photon numbers of the two cavities $Q_L[k] = Q_R[k]$ and $Q_L[-k] = Q_R[-k]$. We discuss the storage effect shown in Fig. 9. When $\frac{\Delta}{\omega_m}$ is around 0.02, $S \approx 1$, which indicates that the system allows photon transfer into the OM cavity $L \to C \leftarrow R$ only. When the transfer is prohibited from the OM cavity $L \leftarrow C \to R$, the photon number in the cavities L and R from the OM cavity is approximately equal to zero. When the second-order correlation $g_C^{(2)}(0) > 1$, photons exhibit a bunching effect in the OM cavity and when $g_R^{(2)}(0) = g_L^{(2)}(0) < 1$, photons exhibit an antibunching effect in the left and right cavities. When the convergence field k is bounded in the OM cavity, the system exhibits a storage characteristic. As shown in Fig. 10, the system exhibits a release characteristic. When $\frac{\Delta}{\omega_m}$ is around 0.007, $S \approx -1$, which indicates that the system allows photon transfer out of the OM cavity $L \leftarrow C \to R$ only. When the second-order correlation $g_C^{(2)}(0) < 1$, photons exhibit an antibunching effect in the OM cavity and when $g_R^{(2)}(0) = g_L^{(2)}(0) > 1$, photons exhibit a bunching effect in the left and right cavities. That is, the divergent field $-k$ is released from the OM cavity. We also notice that when $\mathcal{S} = 1$ and $\mathcal{M}_S = 1$, complete storage is indicated, whether the field from the left or the right cavity can be stored in the OM cavity, which is similar to the capacitor charge process. When $\mathcal{S} = -1$ and $\mathcal{M}_R = 1$, complete release is indicated and the field in the OM cavity can be released through the left and right cavities completely, which is similar to the capacitor discharge process. The two processes can be controlled by the detuning of the driving field Δ. In contrast, like the filter effect, there is no photon in the channel at the frequency that let $\mathcal{S} = 1$ and $\mathcal{M}_S = 1$ (complete absorption), but this has no effect on the frequency that let $\mathcal{S} = -1$ and $\mathcal{M}_R = 1$ (complete release).

In the previous discussion we ignored the effects of the mechanical thermal bath. Now, to investigate the influence of the mechanical thermal temperature on the correlation function, we include the mechanical thermal reservoir. Using the master equation (4), in Fig. 11 we plot the minimum values of $g_L^2(0)$ as a function of the reservoir temperature; the $g_L^2(0)$ versus $\frac{\Delta}{\omega_m}$ affected by the thermal reservoir is also displayed in the inset. When the temperature is below 1 mK (marked with the shadow area), the thermal heating has nearly no effect in Fig. 11(a), because when the influence of the mechanical bath is far below the single-photon coupling rate, i.e., $\gamma n_{th} \ll g$, the bath effect can be ignored. With current experimental techniques, one can easily set $g/\gamma \gg 1$ [36,37], which means that a small value of the phonon number n_{th} can be tolerated with little effect. Also, we can clearly see that the antibunching effect becomes weaker with increasing temperature. In the UPB regime, as shown in Fig. 11(b), the antibunching effect is more sensitive to the bath temperature. This quantum effect will disappear when the temperature is over 5 mK ($n_{th} = 0.62$). Fortunately, the current experimental conditions of ground-state cooling can achieve $n_{th} = 0.34 \pm 0.05$ [22]. This provides some resistance to the quantum decoherence of our system. Even so, to maintain the antibunching effect, the mechanical thermal noise still needs to be suppressed.

IV. CONCLUSION

In this paper we employed radiation pressure and destructive interference effects to construct the controller of photon transport. By coupling the cavity of an optomechanical system to two cavities, we show that the photon blockade can be achieved in the single-photon strong-coupling regime

and the single-photon weak-coupling regime. In the single-photon strong-coupling regime, the photon blockade effect mainly results from the nonlinearity of the radiation pressure in the optomechanical cavity, while in the single-photon weak-coupling regime, the photon blockade effect is mainly because of the interference between multiple paths for two-photon excitation in cavities. For few-photon control of one-dimensional transmission, the system can work as an optical diode without the requirement of the strength of the radiation pressure strong coupling and the rectification of photons can be controlled by the detuning of the driving field Δ. If we just drive the cavity from the left or right cavity only, the system can function as a single-photon source. Furthermore, when two fields are transported into the OM cavity through the cavities L and R, the device can store and release photons as a capacitor in an appropriate parameter regime. These properties provide a promising application of the optomechanical system in quantum information processing and quantum circuit realization.

ACKNOWLEDGMENT

This work was supported by NSFC under Grant No. 11474044.

APPENDIX: SOLUTION OF THE PROBABILITY AMPLITUDES

If we set $\kappa_L = \kappa_R = \kappa_C = \kappa$ and $\omega_m \gg g$ and adiabatically eliminate the degree of the oscillators, we can obtain the equations of motion of the probability amplitudes under the weak-pumping regime $C_0 \gg C_{s1} \gg C_{s1s2}$. We drop higher-order terms in the zero- and one-photon probability amplitudes

$$
\begin{aligned}
i\dot{C}_L &= \alpha_L C_L + \varepsilon_L C_0 + J_L C_C,\\
i\dot{C}_C &= (\alpha_C + \delta) C_C + \varepsilon_C C_0 + J_L C_L + J_R C_R,\\
i\dot{C}_R &= \alpha_R C_R + \varepsilon_R C_0 + J_R C_C,\\
i\dot{C}_{LC} &= (\alpha_L + \alpha_C + \delta) C_{LC} + \varepsilon_L C_C + \varepsilon_C C_L + \sqrt{2} J_L (C_{LL} + C_{CC}) + J_R C_{LR},\\
i\dot{C}_{LR} &= (\alpha_L + \alpha_R) C_{LR} + \varepsilon_L C_R + \varepsilon_R C_L + J_L C_{CR} + J_R C_{LC},\\
i\dot{C}_{CR} &= (\alpha_R + \alpha_C + \delta) C_{CR} + \varepsilon_C C_R + \varepsilon_R C_C + \sqrt{2} J_R (C_{RR} + C_{CC}) + J_L C_{LR},\\
i\dot{C}_{LL} &= 2\alpha_L C_{LL} + \sqrt{2}\varepsilon_L C_L + \sqrt{2} J_L C_{LC},\\
i\dot{C}_{CC} &= (2\alpha_C + 4\delta) C_{CC} + \sqrt{2}\varepsilon_C C_C + \sqrt{2} J_L C_{LC} + \sqrt{2} J_R C_{CR},\\
i\dot{C}_{RR} &= 2\alpha_R C_{RR} + \sqrt{2}\varepsilon_R C_R + \sqrt{2} J_R C_{CR},
\end{aligned}
\tag{A1}
$$

where $\alpha_L = \Delta_L - i\kappa/2$, $\alpha_R = \Delta_R - i\kappa/2$, and $\alpha_C = \Delta_C - \kappa/2 + \delta$. If we set the initial state as a vacuum state, i.e., $C_0(0) = 1$, $C_{s1}(0) = C_{s1s2}(0) = 0$, where $\{s1,s2\} \in \{L,C,R\}$. In the weak-driving regime $\{\varepsilon_C/\kappa_C, \varepsilon_L/\kappa_L, \varepsilon_R/\kappa_R\} \ll 1$, the photon number is small, so we have $C_0(\infty) \approx C_0(0)$ and then the long-time solution of equations can be approximately obtained as

$$C_L = \frac{\left[-J_R^2 + \alpha_R(\alpha_C + \delta)\right]\varepsilon_L + J_L(-\alpha_R\varepsilon_C + J_R\varepsilon_R)}{D_1}, \tag{A2}$$

$$C_C = \frac{\alpha_L\alpha_R\varepsilon_C - J_L\alpha_R\varepsilon_L - J_R\alpha_L\varepsilon_R}{D_1}, \tag{A3}$$

$$C_R = \frac{\left[-J_L^2 + \alpha_L(\alpha_C + \delta)\right]\varepsilon_R + J_R(-\alpha_L\varepsilon_C + J_L\varepsilon_L)}{D_1}, \tag{A4}$$

$$C_{LL} = \frac{C_L \sum_{j=(L,C,R)} l_{L,j}\varepsilon_j + J_L C_C \sum_{j=(L,C,R)} l_{C,j}\varepsilon_j + J_L J_R C_R \sum_{j=(L,C,R)} l_{R,j}\varepsilon_j}{\sqrt{2} D_2}, \tag{A5}$$

$$C_{CC} = \frac{J_L C_L \sum_{j=(L,C,R)} c_{L,j}\varepsilon_j + C_C \sum_{j=(L,C,R)} c_{C,j}\varepsilon_j + J_R C_R \sum_{j=(L,C,R)} c_{R,j}\varepsilon_j}{\sqrt{2} D_2}, \tag{A6}$$

$$C_{RR} = \frac{J_L J_R C_L \sum_{j=(L,C,R)} r_{L,j}\varepsilon_j + J_R C_C \sum_{j=(L,C,R)} r_{C,j}\varepsilon_j + C_R \sum_{j=(L,C,R)} r_{R,j}\varepsilon_j}{\sqrt{2} D_2}, \tag{A7}$$

where the first term in Eq. (A5) describes two-photon state generated by the driving field in the cavity L, the second term describes two-photon excitation due to photon tunneling between the OM cavity and the left cavity with coupling rate J_L, and the third term describes two-photon excitation due to photon tunneling between the right cavity and left cavity through the OM cavity. When the collective effect of the three processes let $C_{LL} \approx 0$, photons exhibit the blockade effect in cavity L. In addition

to Eqs. (A6) and (A7) we have

$$
\begin{aligned}
D_1 &= J_L^2\alpha_L + J_R^2\alpha_R - \alpha_L\alpha_R(\alpha_C+\delta),\\
D_2 &= \sum_{s=L,R}\alpha_s\big[J_s^2-\alpha_s(\alpha_s+\alpha_C+\delta)\big]\big[2J_s^2(\alpha_s+\alpha_C+2\delta)-\alpha_s(\alpha_s+\alpha_C+\delta)(\alpha_C+2\delta)\big],\\
l_{L,L} &= J_L^4\alpha_R + \big[J_R^2-(\alpha_L+\alpha_R)(\alpha_C+\alpha_L+\delta)\big]\big[-\alpha_R(\alpha_C+\alpha_R+\delta)(\alpha_C+2\delta)+J_R^2(\alpha_C+\alpha_R+2\delta)\big]\\
&\quad + J_L^2\big\{J_R^2(\alpha_L-\alpha_R)-\alpha_R\big[\alpha_C^2+\alpha_R(\alpha_L+\alpha_R)+(3\alpha_L+\alpha_R)\delta+2\delta^2+\alpha_C(2\alpha_L+\alpha_R+3\delta)\big]\big\},\\
l_{L,C} &= J_L\big\{J_R^2(\alpha_L+\alpha_R)(\alpha_C+\alpha_R+2\delta)-\alpha_R(\alpha_C+2\delta)\big[-J_L^2+(\alpha_L+\alpha_R)(\alpha_C+\alpha_R+\delta)\big]\big\},\\
l_{L,R} &= J_LJ_R\big\{-J_R^2(\alpha_C+\alpha_R+2\delta)+\alpha_R\big(J_L^2+(\alpha_C+\alpha_R+\delta)(\alpha_C+2\delta)\big)\big]\big\},\\
l_{C,L} &= -J_R^2(\alpha_L+\alpha_R)(\alpha_C+\alpha_R+2\delta)+\alpha_R(\alpha_C+2\delta)\big[-J_L^2+(\alpha_L+\alpha_R)(\alpha_C+\alpha_R+\delta)\big],\\
l_{C,C} &= J_L\big[J_R^2\alpha_L+J_L^2\alpha_R-\alpha_R(\alpha_L+\alpha_R)(\alpha_C+\alpha_R+\delta)\big],\\
l_{C,R} &= J_LJ_R\alpha_R(\alpha_C+\alpha_L+\alpha_R+2\delta),\\
l_{R,L} &= J_R^2(\alpha_C+\alpha_R+2\delta)-\alpha_R\big[J_L^2+(\alpha_C+\alpha_R+\delta)(\alpha_C+2\delta)\big],\\
l_{R,C} &= J_L\alpha_R(\alpha_C+\alpha_L+\alpha_R+2\delta),\\
l_{R,R} &= -J_LJ_R(\alpha_C+\alpha_L+\alpha_R+2\delta),\\
c_{L,L} &= J_L\big[J_R^2\alpha_L+J_L^2\alpha_R-\alpha_R(\alpha_L+\alpha_R)(\alpha_C+\alpha_R+\delta)\big],\\
c_{L,C} &= \alpha_L\big[-J_R^2\alpha_L-J_L^2\alpha_R+\alpha_R(\alpha_L+\alpha_R)(\alpha_C+\alpha_R+\delta)\big],\\
c_{L,R} &= J_R\big\{J_R^2\alpha_L-\alpha_R[-J_L^2+\alpha_L(2\alpha_C+\alpha_L+\alpha_R+2\delta)]\big\},\\
c_{C,L} &= J_L\alpha_L\big[-J_R^2\alpha_L-J_L^2\alpha_R+\alpha_R(\alpha_L+\alpha_R)(\alpha_C+\alpha_R+\delta)\big],\\
c_{C,C} &= -J_L^4\alpha_R-\alpha_L\big[J_R^2-(\alpha_L+\alpha_R)(\alpha_C+\alpha_L+\delta)\big]\big[J_R^2-\alpha_R(\alpha_C+\alpha_R+\delta)\big]\\
&\quad + J_L^2\big\{-J_R^2(\alpha_L+\alpha_R)+\alpha_R\big[\alpha_L^2+\alpha_C(2\alpha_L+\alpha_R)+\alpha_R(\alpha_R+\delta)+\alpha_L(\alpha_R+2\delta)\big]\big\},\\
c_{C,R} &= J_R\alpha_R\big[-J_R^2\alpha_L-J_L^2\alpha_R+\alpha_L(\alpha_L+\alpha_R)(\alpha_C+\alpha_L+\delta)\big],\\
c_{R,L} &= J_L\big\{J_R^2\alpha_L-\alpha_R\big[-J_L^2+\alpha_L(2\alpha_C+\alpha_L+\alpha_R+2\delta)\big]\big\},\\
c_{R,C} &= \alpha_R\big[-J_R^2\alpha_L-J_L^2\alpha_R+\alpha_L(\alpha_L+\alpha_R)(\alpha_C+\alpha_L+\delta)\big],\\
c_{R,R} &= J_R\big[J_R^2\alpha_L+J_L^2\alpha_R-\alpha_L(\alpha_L+\alpha_R)(\alpha_C+\alpha_L+\delta)\big],\\
r_{i,j} &= l_{i,j}(J_L\leftrightarrow J_R,\alpha_L\leftrightarrow\alpha_R)\quad (i,j=\{L,C,R\}).
\end{aligned}
\tag{A8}
$$

The second-order correlation functions with zero time delay are

$$
\begin{aligned}
g_L^{(2)}(0) &= \frac{2|C_{LL}|^2}{(|C_L|^2+|C_{LC}|^2+|C_{LR}|^2+2|C_{LL}|^2)^2}\approx\frac{2|C_{LL}|^2}{|C_L|^4},\\
g_C^{(2)}(0) &= \frac{2|C_{CC}|^2}{(|C_C|^2+|C_{LC}|^2+|C_{CR}|^2+2|C_{CC}|^2)^2}\approx\frac{2|C_{CC}|^2}{|C_C|^4},\\
g_R^{(2)}(0) &= \frac{2|C_{RR}|^2}{(|C_R|^2+|C_{CR}|^2+|C_{LR}|^2+2|C_{RR}|^2)^2}\approx\frac{2|C_{RR}|^2}{|C_R|^4}.
\end{aligned}
\tag{A9}
$$

The mean occupation numbers of the three cavities are

$$
\begin{aligned}
N_L &= (|C_L|^2+|C_{LC}|^2+|C_{LR}|^2+2|C_{LL}|^2)N_0\approx|C_L|^2N_0,\\
N_C &= (|C_C|^2+|C_{LC}|^2+|C_{CR}|^2+2|C_{CC}|^2)N_0\approx|C_C|^2N_0,\\
N_R &= (|C_R|^2+|C_{CR}|^2+|C_{LR}|^2+2|C_{RR}|^2)N_0\approx|C_R|^2N_0,
\end{aligned}
\tag{A10}
$$

where $N_0=(\varepsilon_L/\kappa_L)^2+(\varepsilon_C/\kappa_C)^2+(\varepsilon_R/\kappa_R)^2$.

[1] K. Stannigel, P. Komar, S. J. M. Habraken, S. D. Bennett, M. D. Lukin, P. Zoller, and P. Rabl, Phys. Rev. Lett. **109**, 013603 (2012).

[2] A. Miranowicz, M. Paprzycka, Y. X. Liu, J. Bajer, and F. Nori, Phys. Rev. A **87**, 023809 (2013).

[3] X.-W. Xu and Y. Li, Phys. Rev. A **90**, 033832 (2014).

[4] H.-Z. Wu, Z.-B. Yang, and S.-B. Zheng, Phys. Rev. A **82**, 034307 (2010).
[5] Y. Han, B. He, K. Heshami, C.-Z. Li, and C. Simon, Phys. Rev. A **81**, 052311 (2010).
[6] F.-Y. Hong and S.-J. Xiong, Phys. Rev. A **78**, 013812 (2008).
[7] J. L. O'Brien, Science **318**, 1567 (2007).
[8] H. A. Haus, *Waves and Fields in Optoelectronics* (Prentice-Hall, Englewood Cliffs, 1984).
[9] K. Gallo, G. Assanto, K. Parameswaran, and M. Fejer, Appl. Phys. Lett. **79**, 314 (2001).
[10] B. E. A. Saleh and M. C. Teich, *Fundamentals of Photonics*, 2nd ed. (Wiley, New York, 2007).
[11] L. Fan, J. Wang, L. T. Varghese, H. Shen, B. Niu, Y. Xuan, A. M. Weiner, and M. Qi, Science **335**, 447 (2011).
[12] M. S. Kang, A. Butsch, and P. S. J. Russell, Nat. Photon. **5**, 549 (2011).
[13] D.-W. Wang, H.-T. Zhou, M.-J. Guo, J.-X. Zhang, J. Evers, and S.-Y. Zhu, Phys. Rev. Lett. **110**, 093901 (2013).
[14] E. Mascarenhas, D. Gerace, D. Valente, S. Montangero, A. Auffves, and M. F. Santos, Europhys. Lett. **106**, 54003 (2014).
[15] H. Z. Shen, Y. H. Zhou, and X. X. Yi, Phys. Rev. A **90**, 023849 (2014).
[16] P. Rabl, Phys. Rev. Lett. **107**, 063601 (2011).
[17] T. Ramos, V. Sudhir, K. Stannigel, P. Zoller, and T. J. Kippenberg, Phys. Rev. Lett. **110**, 193602 (2013).
[18] G. S. Agarwal and S. Huang, Phys. Rev. A **81**, 041803 (2010).
[19] J. D. Teufel, D. Li, M. S. Allman, K. Cicak, A. J. Sirois, J. D. Whittaker, and R. W. Simmonds, Nature (London) **471**, 204 (2011).
[20] S. Aldana, C. Bruder, and A. Nunnenkamp, Phys. Rev. A **88**, 043826 (2013).
[21] L. Zhou, J. Cheng, Y. Han, and W. Zhang, Phys. Rev. A **88**, 063854 (2013).
[22] J. D. Teufel, T. Donner, D. Li, J. W. Harlow, M. S. Allman, K. Cicak, A. J. Sirois, J. D. Whittaker, K. W. Lehnert, and R. W. Simmonds, Nature (London) **475**, 359 (2011).
[23] J. Chan, T. P. M. Alegre, A. H. Safavi-Naeini, J. T. Hill, A. Krause, S. Gröblacher, M. Aspelmeyer, and O. Painter, Nature (London) **478**, 89 (2011).
[24] B. Abbott *et al.*, New J. Phys. **11**, 073032 (2009).
[25] A. Pontin, M. Bonaldi, A. Borrielli, F. S. Cataliotti, F. Marino, G. A. Prodi, E. Serra, and F. Marin, Phys. Rev. A **89**, 023848 (2014).
[26] M. Aspelmeyer, T. J. Kippenberg, and F. Marquardt, Rev. Mod. Phys. **86**, 1391 (2014).
[27] W. Z. Jia and Z. D. Wang, Phys. Rev. A **88**, 063821 (2013).
[28] X. X. Ren, H. K. Li, M. Y. Yan, Y. C. Liu, Y. F. Xiao, and Q. Gong, Phys. Rev. A **87**, 033807 (2013).
[29] J.-Q. Liao and F. Nori, Phys. Rev. A **88**, 023853 (2013).
[30] X.-Y. Lü, W.-M. Zhang, S. Ashhab, Y. Wu, and F. Nori, Sci. Rep. **3**, 2943 (2013).
[31] D. Hu, S.-Y. Huang, J.-Q. Liao, L. Tian, and H.-S. Goan, Phys. Rev. A **91**, 013812 (2015).
[32] M. Bamba, A. Imamoğlu, I. Carusotto, and C. Ciuti, Phys. Rev. A **83**, 021802 (2011).
[33] C. W. Gardner and P. Zoller, *Quantum Noise* (Springer, Berlin, 2000).
[34] T. C. H. Liew and V. Savona, Phys. Rev. Lett. **104**, 183601 (2010).
[35] X.-W. Xu and Y. Li, Phys. Rev. A **90**, 043822 (2014).
[36] K. W. Murch, K. L. Moore, S. Gupta, and D. M. Stamper-Kurn, Nat. Phys. **4**, 561 (2008).
[37] D. Kleckner, B. Pepper, E. Jeffrey, P. Sonin, S. M. Thon, and D. Bouwmeester, Opt. Express **19**, 19708 (2011).